# Hermitian non-Markovian stochastic master equations for quantum dissipative dynamics

Yun-An Yan and Yun Zhou

*Guizhou Provincial Key Laboratory of Computational Nano-Material Science, Guizhou Normal College, Guizhou 550018, China*

(Received 30 January 2015; published 24 August 2015)

It remains a challenge for theory to simulate nonperturbative and non-Markovian quantum dissipative dynamics at low temperatures. In this study we suggest a Hermitian non-Markovian stochastic master equation suitable for dissipative dynamics at arbitrary temperatures. The memory effect of the bath is embedded within two real correlated Gaussian noises. This scheme is numerically verified by the hierarchical equation of motion and symmetry preserving for a symmetric two-level system. An exemplary application is carried out for the dynamics over a broad range of temperatures to investigate the temperature dependence of the Rabi frequency shift and the non-Markovianity.

DOI: 10.1103/PhysRevA.92.022121 PACS number(s): 03.65.Yz, 05.10.Gg, 05.40.−a, 05.70.Ln

## I. INTRODUCTION

A quantum system is inevitably coupled to its environment. When the coupling is weak and the memory time of the environment is short compared to the system time, a Markovian approximation leads to a good description. However, experiments have depicted that the Markovian approximation fails to describe the dynamics of various quantum systems in physics, chemistry, and biology [1–3]. The interest in non-Markovian dynamics is thus renewed [4–10].

To deal with dissipative dynamics, it is a widely accepted assumption that the bath is consisted with independent quantum harmonic oscillators linearly coupled to the system within the framework of system-bath separation, which is normally called the Caldeira-Leggett model [11]. With this approach, the impact of the bath on the system is fully characterized by its response function. The Caldeira-Leggett model has become the standard model for the theoretical description of quantum dissipation and continues to receive attentions, such as the hierarchy of equations of multiple-time correlation functions [12], time-convolutionless master equations for non-Markovian dynamics for two-level systems (TLSs) [13,14], and effect of the initial system-environment correlations [15], to name but a few.

The stochastic method is useful for attacking quantum dissipative dynamics, partially because the Feynman-Vernon's influence functional [16] based on the Caldeira-Leggett model provides a natural measure for stochastic processes. Percival and coworkers have done pioneering work with stochastic unraveling in the Markovian case [17]. For non-Markovian dynamics, the direct implementation of the above observation led to many further developments, with the quantum Monte Carlo method [18] and the quasiadiabatic propagator path integral approach [19] being two successful examples.

However, the quantum Monte Carlo is only suitable for short-time dynamics due to the numerical sign problem, and the quasiadiabatic propagator path integral method is only good for short memory cases. A more efficient strategy is to derive a stochastic differential equation (SDE) for the dissipative dynamics by decoupling the influence functional. In this case there are two key factors affecting the numerical performance of the SDE. One is the number of stochastic processes in the SDE, which is obvious and is not discussed in further detail. The other is the extent of the stochastic reduced density matrix (SRDM) to preserve the general and problem-specific properties of the reduced density matrix (RDM). Here the general properties refer to the norm conservation, the hermicity, and the positivity of the RDM, and the problem-specific properties, to the symmetry properties of the system. The SRDM will not necessarily preserve these properties, although its stochastic average has to do so. Generally speaking, the more properties of the RDM the SRDM preserves, the better numerical performance the SDE method will assume.

One can decouple the whole system-bath interaction in terms of stochastic processes and reach the SDE for reduced dynamics. This idea was carried out by Shao [20] and Stockburger *et al.* [21–23] independently using different strategies. These two approaches are equivalent as far as the Caldeira-Leggett model is concerned. Please note that Shao's approach can go beyond the linear dissipation model and may apply to an arbitrary system-bath interaction and arbitrary bath. Also, starting from Shao's approach, one of us and coworkers have been the first to rigorously derive the hierarchical equation of motion (HEOM) [24,25], which was originally proposed by Tanimura and Kubo as the semiclassical approximation for high-temperature dissipative dynamics [26]. The SDE is non-Hermitian and has three real stochastic processes. Thus if written in the language of wave-function description, the forward propagation and backward propagation satisfy different sets of equations which are not Hermitian conjugated to each other. The non-Hermitian nature of the SDE affects the numerical performance and thus its application as a numerical tool is limited.

One can also partially decouple the influence functional to get a Hermitian SDE. Strunz, Yu, and coworkers only decoupled the coupling between the forward and the backward paths in the influence functional and put forward a stochastic Schrödinger equation for open systems, called the non-Markovian quantum state diffusion (NMQSD) equation [27–32]. It is a Hermitian SDE and thus assumes a much better numerical performance. But it contains an unknown kernel, which can only be determined self-consistently by assuming some ansatz. The kernel is only explicitly solvable for some special cases and one has to solve it case by case [33,34] or with the functional expansion [35]. The lack of an explicit expression of the kernel and a straightforward way to solve it

 

hinders the application of the NMQSD method to most general cases.

This work presents a Hermitian non-Markovian stochastic master equation (SME) for the RDM with two real correlated colored noises. On one hand, the hermicity and lower number of noises will make the current scheme more efficient numerically than that proposed by Stockburger *et al.* [22] and Shao [20]. On the other hand, this Hermitian SME does not contain unknown kernels and is much easier to implement than NMQSD for all kinds of applications [27]. It thus partially overcomes the shortcomings of the above-mentioned stochastic approaches and is suitable for long-time dynamics at arbitrary temperatures. The rest of the paper is organized as follows. Section II gives the theoretical derivation of the Hermitian SME. Preliminary results for the temperature-dependent dynamics of a symmetric TLS are carried out in Sec. III. Section IV gives a brief summary.

## II. HERMITIAN STOCHASTIC DIFFERENTIAL EQUATION

This work focuses on the linear dissipation dictated by the Caldeira-Leggett model,

$$\hat{H} = \hat{H}_s + \hat{H}_b + f(\hat{s})g(\hat{b}), \quad g(\hat{b}) = \sum_j c_j \hat{x}_j, \tag{1}$$

where $\hat{H}_s$ and $\hat{H}_b$ are the Hamiltonians of the subsystem of interest and the heat reservoir, respectively. $\hat{s}$ is the system operator coupled to the bath, while $\hat{x}_j$ is the position operator of the $j$th mode in the environment.

As the sole quantity needed for the bath is its response function, different methods will be equivalent to each other as long as they can represent the response function correctly. The stochastic decoupling scheme is the simplest among various schemes for accomplishing this task. The SDE originally proposed by Shao in Ref. [20] can decouple the dissipative interaction,

$$\begin{aligned} i\hbar d\hat{\rho}_s &= [\hat{H}_s,\hat{\rho}_s]dt + \sqrt{\hbar/2}[f(\hat{s}),\hat{\rho}_s]d\mu_2 \\ &\quad + i\sqrt{\hbar/2}\{f(\hat{s}),\hat{\rho}_s\}d\mu_1, \end{aligned} \tag{2}$$

$$\begin{aligned} i\hbar d\hat{\rho}_b &= [\hat{H}_b,\hat{\rho}_b]dt + \sqrt{\hbar/2}[g(\hat{b}),\hat{\rho}_b]d\mu_1 \\ &\quad + i\sqrt{\hbar/2}\{g(\hat{b}),\hat{\rho}_b\}d\mu_2, \end{aligned} \tag{3}$$

if the initial condition is deterministic and factorized as $\hat{\rho}_{\rm tot}(0) = \hat{\rho}_s(0)\hat{\rho}_b(0)$. Generally, $\hat{\rho}_s(0)$ is taken according to the process under investigation and $\hat{\rho}_b(0)$ is the Boltzmann distribution with respect to the bath Hamiltonian $\hat{H}_b$. In the above equation $\mu_a (a = 1,2)$ are two classical Wiener processes with the properties

$$\mathcal{M}\langle d\mu_{a,t}\rangle = 0, \quad \mathcal{M}\langle d\mu_{a,t} d\mu_{b,t}\rangle = \delta_{ab} dt. \tag{4}$$

Here $\delta_{ab}$ is the Kronecker $\delta$ function. $\hat{\rho}_s$ is the SRDM for the system of interest. Please note that in this work the SDE is in the Itô sense and the stochastic integral is the Itô integral as well. The full dynamics of the dissipative system is recovered by the stochastic average of the stochastic density matrix $\hat{\rho}_{\rm tot} = \mathcal{M}\langle\hat{\rho}_s\hat{\rho}_b\rangle$, with $\mathcal{M}$ meaning the stochastic average over the two Wiener processes. This point can be justified by using Eq. (4) and the fact that $\hat{\rho}_{s/b}(t)$ is independent of $d\mu_{a,t}$ due to the Itô nature of the SDE. And the RDM will be obtained through the stochastic average after tracing over the bath degrees of freedom, i.e., $\tilde{\rho}_s = \mathcal{M}\langle\hat{\rho}_s \mathrm{tr}(\hat{\rho}_b)\rangle$.

Equation (2) is Hermitian, so is expected to have a much better performance compared to a non-Hermitian one once the trace of the bath $\mathrm{tr}(\hat{\rho}_b)$ is solved. However, the factorization condition for the bath $\hat{\rho}_b = \prod_j \hat{\rho}_{b,j}$ ($j$ refers to the bath degree of freedom) is destroyed and the modes in the bath do not evolve independently of each other. Hence the trace from Eq. (3) cannot be known straightforwardly. To remedy this problem, one may take an alternative way to calculate the trace by introducing two more real Wiener processes $\mu_{3,4}$ and using the following SDE for the bath instead:

$$\begin{aligned} i\hbar d\tilde{\rho}_b &= [\hat{H}_b,\tilde{\rho}_b]dt + \sqrt{\hbar/2}[g(\hat{b}),\tilde{\rho}_b](d\mu_1 + id\mu_4) \\ &\quad + i\sqrt{\hbar/2}\{g(\hat{b}),\tilde{\rho}_b\}(d\mu_2 + id\mu_3). \end{aligned} \tag{5}$$

One can steadily verify that Eqs. (2) and (5) also yield the Liouville equation for the whole dissipative system. Once the trace of $\tilde{\rho}_b$ in Eq. (5) is solved, one knows that in Eq. (3) by averaging over the stochastic processes $\mu_{3,4}$; that is, $\mathrm{tr}(\hat{\rho}_b) = \mathcal{M}_{3,4}(\mathrm{tr}(\tilde{\rho}_b))$. To proceed, one invokes the formal solution of Eq. (5);

$$\begin{aligned} \tilde{\rho}_b(t) &= e_+^{-\frac{i}{\hbar}\int_0^t [\hat{H}_b d\tau + g(\hat{b}) dq_\tau^+]} e^{-\beta\hat{H}_b}/\mathrm{Tr}(e^{-\beta\hat{H}_b}) \\ &\quad \times e_-^{\frac{i}{\hbar}\int_0^t [\hat{H}_b d\tau + g(\hat{b}) dq_\tau^-]}, \end{aligned} \tag{6}$$

where $e_+$ and $e_-$ denote the time and antitime ordering exponentials, respectively, and $q^+$ and $q^-$ are the forward and backward paths:

$$\begin{aligned} q^+ &= \sqrt{\hbar/2}(\mu_1 + i\mu_4 + i\mu_2 - \mu_3), \\ q^- &= \sqrt{\hbar/2}(\mu_1 + i\mu_4 - i\mu_2 + \mu_3). \end{aligned}$$

The trace of the bath in the above equation can be known from the influence functional,

$$\begin{aligned} \mathrm{tr}(\tilde{\rho}_b(t)) = \mathcal{F}[q^+,q^-] = \exp\Bigg\{ &-\frac{1}{\hbar}\int_0^t (dq_\tau^+ - dq_\tau^-) \\ &\times \int_0^\tau [\alpha_R(\tau - s)(dq_s^+ - dq_s^-) \\ &+ i\alpha_I(\tau - s)(dq_s^+ + dq_s^-)]\Bigg\}, \end{aligned}$$

which leads to the following expression for the trace:

$$\begin{aligned} \mathrm{tr}(\tilde{\rho}_b(t)) = \exp\Bigg\{ &2\int_0^t (d\mu_{2,\tau} + id\mu_{3,\tau}) \\ &\times \int_0^\tau [\alpha_R(\tau - s)(d\mu_{2,s} + id\mu_{3,s}) \\ &+ \alpha_I(\tau - s)(d\mu_{1,s} + id\mu_{4,s})]\Bigg\}. \end{aligned}$$

The stochastic average over the Wiener processes $\mu_3$ and $\mu_4$ actually is a Gaussian-type functional integration,

$$\begin{aligned} \mathcal{M}_{3,4}\mathrm{tr}[\tilde{\rho}_b(t)] = \int \mathcal{D}[\mu_3]\mathcal{D}[\mu_4] \exp\Bigg\{ &-\frac{1}{2}\sum_{a=3}^{4}\int_0^t d\mu_{a,\tau} \\ &\times \int_0^t \delta(\tau - s) d\mu_{a,s}\Bigg\} \mathrm{tr}[\tilde{\rho}_b(t)]. \end{aligned} \tag{7}$$

Here $\delta$ is the Dirac $\delta$ function. The functional integration in the above equation is straightforward. Performing a few rearrangements after the integration one finally gets the trace of the matrix $\hat{\rho}_b$,

$$\mathrm{tr}(\hat{\rho}_b) = e^{\frac{1}{2}\sum_{a,b=1}^{2}\int_0^t d\mu_{a,\tau}\int_0^t[\delta_{ab}\delta(\tau-s)-\frac{1}{2}G_{ab}(\tau-s)]d\mu_{b,s}}, \quad (8)$$

where $G(t-\tau)$ is the Green's function for the matrix function $\Gamma(t-\tau)$,

$$\Gamma = \begin{pmatrix} c\delta(t-\tau)+\alpha_R(t-\tau) & \Theta(t-\tau)\alpha_I(t-\tau) \\ \Theta(\tau-t)\alpha_I(\tau-t) & c\delta(t-\tau) \end{pmatrix}, \quad (9)$$

with $c = 1/2$ and $\Theta$ the Heaviside step function, taking values of 0 (1) for $x \leqslant 0$ ($x > 0$). Equation (8) gives the trace for the stochastic density matrix of the bath in Eq. (3) and it is still of the Gaussian form, which serves as a multiplicative factor in the stochastic average for calculating $\tilde{\rho}_s$. In performing the stochastic average over the Wiener process $\mu_{1,2}$ to obtain the RDM, the first term in Eq. (8) cancels with the measure of $\mu_{1,2}$; i.e.,

$$\begin{aligned}\tilde{\rho}_s &= \int \mathcal{D}[\mu_1]\mathcal{D}[\mu_2] e^{-\frac{1}{2}\sum_{a=1}^{2}\int_0^t d\mu_{a,\tau}\int_0^t \delta(\tau-s)d\mu_{a,s}} \hat{\rho}_s(t)\mathrm{tr}(\hat{\rho}_b) \\ &= \int \mathcal{D}[\mu_1]\mathcal{D}[\mu_2] e^{-\frac{1}{4}\sum_{a,b=1}^{2}\int_0^t d\mu_{a,\tau}\int_0^t G_{ab}(\tau-s)d\mu_{b,s}} \hat{\rho}_s(t).\end{aligned}$$

Here the exponential factor is still Gaussian and can be treated as the measure of Gaussian noises. Adopting the change of variables according to $\mu_{a,t} = \sqrt{2}\int_0^t \nu_{a,\tau}d\tau$ ($a = 1,2$), the Itô SDE for the random RDM with respect to the stochastic processes $\nu_{a,t}$ is given by

$$i\hbar\dot{\hat{\rho}}_s = [\hat{H}_s,\hat{\rho}_s] + \sqrt{\hbar}[f(\hat{s}),\hat{\rho}_s]\nu_2 + i\sqrt{\hbar}\{f(\hat{s}),\hat{\rho}_s\}\nu_1. \quad (10)$$

Equation (9) becomes the correlation function for $\nu_a$ with $\mathcal{M}\langle\nu_{a,t}\rangle = 0$ and $\mathcal{M}\langle\nu_{a,t}\nu_{b,\tau}\rangle = \Gamma_{ab}(t-\tau)$.

In the stochastic simulation of the quantum dissipative dynamics, only the RDM, i.e., the expectation of the SRDM in Eq. (10), is of concern and the information for the higher momenta of the SRDM is not needed at all. Thus the constant $c$ in Eq. (9) can be arbitrarily chosen as long as the correlation function is semipositive definite. To prove this point, one introduces the Itô SDE,

$$\begin{aligned}i\hbar\dot{\hat{\rho}}_s &= [\hat{H}_s,\hat{\rho}_s] + \sqrt{\hbar}[f(\hat{s}),\hat{\rho}_s](\nu_2+\nu_4) \\ &\quad + i\sqrt{\hbar}\{f(\hat{s}),\hat{\rho}_s\}(\nu_1+\nu_3), \end{aligned} \quad (11)$$

where $\nu_1$ and $\nu_2$ are Gaussian noises given in Eq. (9), $\nu_3$ and $\nu_4$ are uncorrelated Gaussian white noises assuming the correlation function $\mathcal{M}\langle\nu_{b,t}\rangle = 0$, and $\mathcal{M}\langle\nu_{b,t}\nu_{b,\tau}\rangle = c'\delta(t-\tau)$, with $b = 3,4$ and $c'$ being a positive real number. All other quantities related to the correlation for $\nu_{3,4}$ are 0. One clearly sees that when the partial stochastic average is carried out over the stochastic processes $\nu_3$ and $\nu_4$, Eq. (11) goes back to Eq. (10). So Eq. (11) is equivalent to Eq. (10) for reproducing the RDM in the description of dissipative dynamics. The second step is the introduction of changes of variables $\nu_1' = \nu_1+\nu_3$, $\nu_2' = \nu_2+\nu_4$, $\nu_3' = \nu_3$, and $\nu_4' = \nu_4$. One finds that $\nu_1'$ and $\nu_2'$ satisfy the correlation function in Eq. (9). Further, the SRDM now is independent of the stochastic processes $\nu_3'$ and $\nu_4'$. In this case the stochastic average over $\nu_3'$ and $\nu_4'$ can be steadily carried out, leading to the same SDE as Eq. (10) and the same form correlation function as Eq. (9), but with the $c$ constant changed to $c+c'$. So different values of $c$ in Eq. (9) yield the same RDM as long as the correlation function is semipositive definite. Since different values of $c$ make a big difference in the performance of the numerical simulation, one always prefers to choose the minimum $c$ value that preserves the semipositivity of the correlation function.

Please note that Eq. (10) does not preserve the norm of the stochastic density matrix, which changes according to the differential equation,

$$d\mathrm{tr}(\hat{\rho}_s) = 2/\sqrt{\hbar}\bar{f}\mathrm{tr}(\hat{\rho}_s)d\nu_1, \quad (12)$$

where $\bar{f} = \mathrm{tr}(f(\hat{s})\bar{\rho}_s)$, with $\bar{\rho}_s$ being the normalized density matrix $\bar{\rho}_s = \hat{\rho}_s/\mathrm{tr}(\hat{\rho}_s)$. The solution of Eq. (12) reads

$$\mathrm{tr}(\hat{\rho}_s) = \exp\left\{2/\sqrt{\hbar}\int_0^t \bar{f}_\tau\nu_{1,\tau}d\tau - 2c/\hbar\int_0^t \bar{f}_\tau^2 d\tau\right\}. \quad (13)$$

The second term in the above equation appears due to the existence of the Dirac $\delta$ function in the correlation function. Then the norm-conserving SDE, Eq. (10), thus turns to be

$$\begin{aligned}i\hbar\dot{\bar{\rho}}_s &= [\hat{H}_s,\bar{\rho}_s] + \sqrt{\hbar}[f(\hat{s}),\bar{\rho}_s]\nu_2 \\ &\quad + i\sqrt{\hbar}\{f(\hat{s})-\bar{f},\bar{\rho}_s\}(\nu_1 - 2c\bar{f}/\sqrt{\hbar}). \end{aligned} \quad (14)$$

When using the above equation, the norm of the SRDM has to be taken into account in the stochastic average. This is conveniently done with a Girsanov transformation without changing the correlation function for $\nu_{1,2}$:

$$\begin{aligned}\nu_{1,t} &\to \nu_{1,t} + 2c/\sqrt{\hbar}\bar{f}_t, \\ \nu_{2,t} &\to \nu_{2,t} + 2/\sqrt{\hbar}\int_0^t d\tau\alpha_I(t-\tau)\bar{f}_\tau. \end{aligned} \quad (15)$$

With the above transformation, the final SDE for the SRDM becomes

$$\begin{aligned}i\hbar\dot{\bar{\rho}}_s &= [\hat{H}_s,\bar{\rho}_s] + i\sqrt{\hbar}\{f(\hat{s})-\bar{f},\bar{\rho}_s\}\nu_1 \\ &\quad + \sqrt{\hbar}[f(\hat{s}),\bar{\rho}_s]\left(\nu_2 + 2/\sqrt{\hbar}\int_0^t d\tau\alpha_I(t-\tau)\bar{f}_\tau\right). \end{aligned} \quad (16)$$

The SMEs, (10) and (16), together with the correlation, Eq. (9), are the central result of this work. There is no unknown kernel in the equations and the memory of the bath is explicitly represented with two correlated Gaussian noises. Both equations are Hermitian and advantageous in numerical applications since hermicity greatly improves the performance for the stochastic simulations. Compared to the formulas obtained by Stockburger *et al.* [22] and Shao [20], the SDEs take the same structure. This is a surprise because one might reasonably expect that a Hermitian SDE will be reached after taking the ensemble average partially over the stochastic process, which induces nonhermicity in Shao's approach, which in turn will dramatically change the structure of the SDE. But the current results seem to imply that this average procedure merely introduces a Dirac $\delta$ function into the correlation without changing the structure of the equation

at all. Moreover, the coefficient of the $\delta$ function is arbitrary as long as the correlation function is semipositive. Based on the above connection the current results seem hard to understand. However, one should bear in mind that there exists an infinite number of stochastic methods which are all equivalent to each other as long as they reproduce the exact evolution of the RDM. Actually, the current approach parallels Stockburger's and Shao's method, not the one derived from it. So the above intuitive expectation is based on the wrong connection between the current and the previous and does not hold here.

Equation (10) is a linear SDE, which is simple to implement and stable in numerics, but not norm conserving. Equation (16) is a nonlinear norm-conserving Itô equation which preserves more properties of the RDM. Together with its hermicity, it allows a possible physical interpretation of the SRDM. Also, Eq. (10) is not a positive map, which could lead to the diagonal matrix elements of the SRDM taking negative values. As a direct consequence, $\mathrm{tr}\hat{\rho}_s$ in Eq. (10) may approach 0, and in this case $\bar{\rho}_s = \hat{\rho}_s/\mathrm{tr}(\hat{\rho}_s)$ is not well defined. Thus one has to make sure that $\mathrm{tr}\hat{\rho}_s = 0$ will not occur for any stochastic trajectory before using the norm-conserving version. Simulations not shown here illustrate that at short times the convergence of the nonlinear version is much better than that of the linear one. Unfortunately, there are always trajectories with $\mathrm{tr}\hat{\rho}_s = 0$ for intermediate to strong dissipation at long times and the application of Eq. (16) becomes problematic.

We would also like to point out that the model in Eq. (1) is special since a factorized system-bath interaction is assumed. The most general form of the Hamiltonian within the framework of linear dissipation is

$$\hat{H}_{\mathrm{tot}} = \hat{H}_s + \hat{H}_b + \sum_j f_j(\hat{s}) g_j(\hat{b}), \tag{17}$$

where $g_j(\hat{b})$ is a linear combination of the bath position and momentum operators. In this case, one may introduce more standard classical Wiener processes $\mu_{j,k}$ to decouple the dissipative interaction [20]:

$$\begin{aligned} i\hbar d\hat{\rho}_s &= [\hat{H}_s, \hat{\rho}_s]dt + \sqrt{\hbar/2}\sum_j [f_j(\hat{s}), \hat{\rho}_s] d\mu_{j,2} \\ &\quad + i\sqrt{\hbar/2}\sum_j \{f_j(\hat{s}), \hat{\rho}_s\} d\mu_{j,1}, \end{aligned} \tag{18}$$

$$\begin{aligned} i\hbar d\hat{\rho}_b &= [\hat{H}_b, \hat{\rho}_b]dt + \sqrt{\hbar/2}\sum_j [g_j(\hat{b}), \hat{\rho}_b](d\mu_{j,1} + i d\mu_{j,4}) \\ &\quad + i\sqrt{\hbar/2}\sum_j \{g_j(\hat{b}), \hat{\rho}_b\}(d\mu_{j,2} + i d\mu_{j,3}). \end{aligned} \tag{19}$$

A Hermitian SDE can also be obtained by following the above derivation since the trace of the bath from Eq. (19) is a Gaussian-type functional and the average over the noises $\mu_{j,3}/\mu_{j,4}$ is a Gaussian functional integration. The procedure is completely parallel to the current formalism and is not discussed any further here.

## III. NUMERICAL SIMULATIONS

### A. Symmetric two-level system

The TLS provides a fruitful test bed for new methods due to its simplicity and importance in physics as well as in chemistry. In this study we investigate the dynamics of a symmetric TLS with the developed method. The Hamiltonian for the whole system is Eq. (1) with $\hat{H}_s = \hbar\Delta\sigma_x$ and $f(\hat{s}) = \sigma_z$. Here $\Delta$ is the tunneling matrix element between the left and the right states and $\sigma_x/\sigma_z$ are the Pauli matrices. The spectral density is assumed to take an Ohmic form with Debye regulation,

$$J(\omega) = \eta\omega\omega_c^2/\left(\omega_c^2 + \omega^2\right),$$

where $\eta$ is the coupling strength and $\omega_c$ the cutoff frequency. Please note that here this form is chosen for a convenient application using the HEOM, which provides benchmarks to verify the stochastic method developed in this work. In principle, the stochastic scheme is capable of handling arbitrary spectral densities, including subohmic and superohmic dissipation [36].

This model cannot be analytically solved without approximation. In the following we use the method of Eq. (10) to solve the population dynamics of the TLS numerically due to its simplicity and numerical stability for an intermediate dissipation strength. The SDE, Eq. (10), is integrated with the order 2 weak Runge-Kutta approximation [37], and two-dimensional correlated noises are generated with the circulant embedding approach [38]. These algorithms are implemented in the Hyshe (Hybrid Stochastic-Hierarchical Equations) package [39], which is the first implementation of the hierarchical method and has been successfully employed to study the first numerical exact hierarchical application [24], hybrid stochastic-hierarchical approach [40], exciton dynamics [25,41], and exciton Seebeck effect [42]. In principle, one may use the Bloch vectors to represent the reduced, auxiliary, and stochastic density matrices and gain an advantage in simulations for TLSs. However, the most recent Hyshe package aims at general-purpose applications and uses the complex-valued density matrix.

In this study, $\Delta$ and $\hbar$ are set to 1. So the energy, frequency, and temperature are in units of $\Delta$, and time in the inverse of $\Delta$. We use a nonadiabatic cutoff, $\omega_c = 4$, with a moderate coupling strength, $\eta = 0.2$, for the numerical simulations. The number of time steps of the stochastic integration is 8192, with a step size of 0.001 and the number of trajectories is 40 million for all simulations at different temperatures. Initially, the system is prepared in the left state $\rho_L(0) = |L\rangle\langle L|$. To verify symmetry breaking due to the average with a finite number of trajectories, simulations starting from the right state $\rho_R(0) = |R\rangle\langle R|$ are also carried out. With these settings, it will take about 20 CPU h, with 16 Intel(R) Xeon(R) E5620 CPUs having a clock speed of 2.40 GHz.

### B. Reliability of the Hermitian SDE

The first step for the numerics is verification of the stochastic method, Eq. (10). The stochastic results at temperatures of 1.0, 2.0, 3.0, 4.0, and 5.0 are compared to the numerical exact values from the HEOM. At the same time, we perform stochastic simulations for temperatures of $10^{-4}$, $10^{-3}$, and

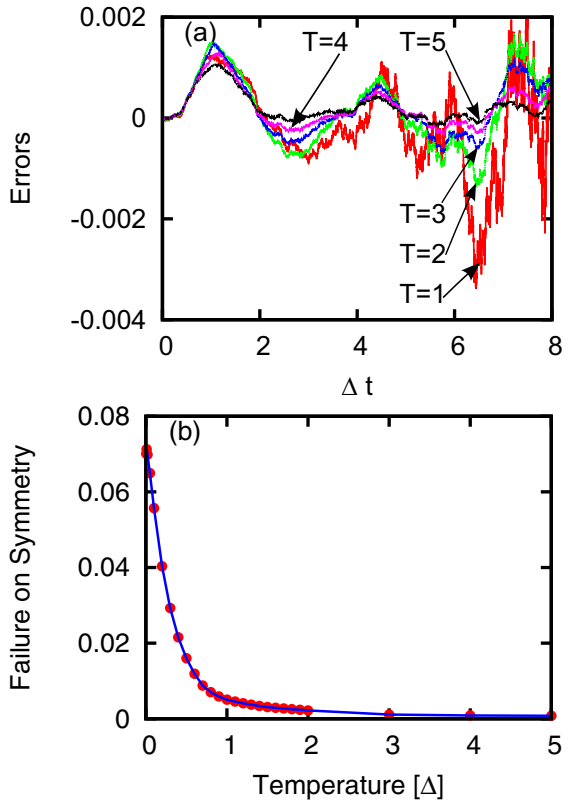


FIG. 1. (Color online) Reliability of the stochastic simulations. (a) Deviations of stochastic simulations from numerical exact hierarchical results; (b) maximum failure of the symmetry preservation measured by the trace distance between a quantum state and its symmetry image at different temperatures. Filled circles represent simulated results and the line is a guide for the eye. The temperature is in units of the tunneling frequency $\Delta$.

$10^{-2}$ and from 0.1 to 2.0 in steps of 0.1 for further analysis. Hierarchical simulations are also carried out at temperatures in the range 2.2–5.0 in steps of 0.2 and the range 6.0–10.0 in steps of 1.0 to save computational effort, thanks to the accuracy and efficiency at high temperatures.

The population difference $P(t)$ between the left and the right states, i.e., the expectation of $\sigma_z$, is a key quantity for checking the dynamics. The quantity $(P_{\rm appr} - P_{\rm real})/(1 + |P_{\rm real}|)$ is a good reference to display the deviation of the approximated value $P_{\rm appr}$ from the real value $P_{\rm real}$. Figure 1(a) presents the errors for population differences, with the converged results from the HEOM being the reference. One finds that the maximum errors are less than 0.004 up to time $t = 8$. If the results from stochastic simulation are plotted on top of the hierarchical ones, the differences cannot be seen with the naked eye. Thus the non-Markovian nonperturbative SME, Eq. (10), produces reliable results. The other main feature is that larger errors occur at lower temperatures, as already noted for the Monte Carlo simulations.

In this model the symmetry between the left and the right states with the symmetry operation $\sigma_x$ are preserved even though the Hamiltonian for the whole system is not invariant under the symmetry operation. The reason is the left-right symmetry of the bath and the symmetry property of the system Hamiltonian as well as the coupling operator,

$$\sigma_x \hat{H}_s \sigma_x = \hat{H}_s, \quad \sigma_x f(\hat{s}) \sigma_x = -f(\hat{s}).$$

So the symmetry operation operator commutes with the propagator of the RDM; i.e., if the condition $\rho_2(t) = \sigma_x \rho_1(t) \sigma_x$ is satisfied at the initial time, it is satisfied at any later time.

It is straightforward to show that the SDE, Eq. (10), preserves the symmetry for the current spin-boson model only after stochastic averaging, but not at the stochastic trajectory level. Thus it is natural to check the reliability of the stochastic simulation with the symmetry-breaking effect due to the stochastic average with a finite number of trajectories in real applications,

$$s(\rho_1(0);t) = D(\rho_1(t), \sigma_x \rho_2(t) \sigma_x), \tag{20}$$

for any initial state $\rho_1(0)$ and its symmetry image $\rho_2(0) = \sigma_x \rho_1(0) \sigma_x$. In the above equation, $D$ is the trace distance of two quantum states $\rho_{1,2}$,

$$D(\rho_1, \rho_2) = \tfrac{1}{2} \mathrm{tr} \sqrt{(\rho_1^\dagger - \rho_2^\dagger)(\rho_1 - \rho_2)}, \tag{21}$$

which is a natural metric in the state space satisfying $0 \leqslant D \leqslant 1$. It is invariant under unitary transformation and nonincreasing for completely positive and trace-preserving quantum maps. Thus the trace distance is often interpreted as a measure for the distinguishability of states. By definition, $s(\rho_1(0),t)$ is semipositive definite and is 0 for $t = 0$. If the symmetry is strictly preserved, $s(\rho_1(0))$ is always 0. In this work we use the maximum value,

$$\mathcal{B}(\rho_1(0)) = \max s(\rho_1(0),t), \tag{22}$$

to check the quality of the stochastic simulation.

Figure 1(b) depicts the failure of the preservation of the left-right symmetry of the system measured as Eq. (22) caused by the finite stochastic average. Since this quantity use the maximum values of the left-right asymmetry as the measure, it normally occurs close to the end time in a stochastic simulation due to the diffusion nature of the SDE, Eq. (10). The overall magnitude of the failure is small. Again, one sees that the lower the temperature is, the larger the error that is induced. Symmetry preservation is a good self-check for the reliability of the method if the benchmark is absent.

### C. Temperature dependence of the dynamics

The temperature dependence of the dynamics is depicted in Fig. 2. Shown is the time evolution of the population difference between the left and the right states. One first observes the decrease in decoherence at higher temperatures. Calculated (but not shown) results for temperatures of 6.0, 7.0, 8.0, 9.0, and 10.0 reveal that for the current setting the population difference will decrease monotonically when the temperature is higher than 6. The second interesting point is that the contour for $\langle \sigma_z \rangle = 0$ is not a straight line. This fact is a reflection of the phenomenon of the change in Rabi frequency at different temperatures. One may define a Rabi oscillation frequency for each temperature based on the population difference in the case of a nonmonotonic decrease. The results are plotted in Fig. 3 together with a quadratic fitting:

$$f(T) = 1.91 + 0.127\,T - 0.330\,T^2. \tag{23}$$

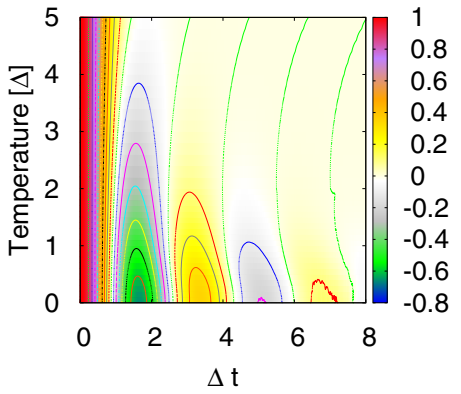


FIG. 2. (Color online) Temperature dependence of the time evolution for the population difference between the left and the right states. Contours are the equi-interval plots with a 0.1 increment of the population difference. The temperature is in units of the tunneling frequency $\Delta$.

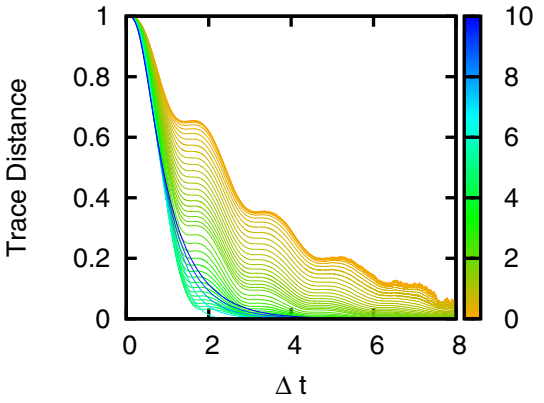


FIG. 4. (Color online) Trace distance between the left and the right states for different temperatures. The temperature for each curve can be read from the color map at the right.

It is clear that the change is not monotonic but convex instead. This trend agrees with various experiments related to TLSs, such as silicon resonators [43], superconducting coplanar waveguide resonators [44], and magnetic dipole radiation in antiferromagnetic $GdFeO_3$ ceramics [45], and theoretical investigation of glasses as well [46,47].

### D. Non-Markovianity based on symmetry

Introduce the rate of change of the trace distance for two states:

$$\sigma(\rho_1(0),\rho_2(0);t) \equiv \frac{d}{dt} D(\rho_1(t),\rho_2(t)). \tag{24}$$

$\sigma$ is always seminegative definite for completely positive and trace-preserving maps and becomes positive only for non-Markovian processes. Breuer, Laine, and Piilo suggested the maximum integrated value for all positive $\sigma$ for all pairs of initial states as the measure for non-Markovianity [9]. It is noteworthy that there exist alternatives for the measure of non-Markovianity, such as the indivisibility property [8,48], quantum Fisher information [49], fidelity [50], singularity of the dynamical map [51], quantum mutual information [5], and local quantum uncertainty [52]. However, it has been observed that there are controversial issues in the measurements [49,53,54]. Interested readers may refer to Ref. [55] for a recent review of the characterization and quantification of non-Markovianity.

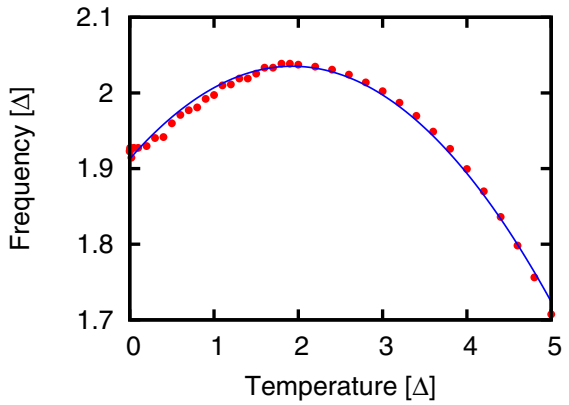


FIG. 3. (Color online) Temperature dependence of the Rabi frequency, which is defined as $\pi$ divided by the position of the first local minimum for the population difference for each temperature. Filled circles represent simulated results; the line, the quadratic fitting of Eq. (23). The temperature is in units of the tunneling frequency $\Delta$.

Generally an accurate measure of non-Markovianity requires complete knowledge of the reduced dynamics, which is only feasible for small systems both in theory and in experiment. Regarding experiments, knowing any effect of the violation of divisibility is already enough to confirm the existence of non-Markovian behavior. It is desired in some applications to know whether or not a particular quantum trajectory is Markovian. This is possible in the presence of symmetry. Then one may introduce a measure of the non-Markovianity for a given quantum trajectory $\rho(t)$ using the trace distance to its symmetry image $\sigma_x\rho(0)\sigma_x$. In this work we use the maximum positive value

$$\mathcal{N} = \max \sigma(\rho_L,\sigma_x\rho_L\sigma_x;t) \tag{25}$$

to check the maximum deviation of the TLS model from Markovianity. Due to the left-right symmetry of the current model, knowing the propagation of either of the two density matrices $\rho_{L/R}$ is sufficient to determine the existence of a non-Markovian effect if a positive $\mathcal{N}$ value is observed. Actually Eq. (25) provides a lower bound for the non-Markovianity measured with the method of Breuer, Laine, and Piilo [49].

The time evolution of the trace distance between $\rho_L(t)$ and $\sigma_x\rho_L(t)\sigma_x$ is present in Fig. 4 for different temperatures. We have also carried out the propagation of $\rho_R(t)$ to check the reliability of the symmetry based method. The differences between the two sets of results are always less than 5% at any time for all temperatures. And the larger errors generally occur close to the end of the propagation time. From this plot one again finds that $T = 6$ is a special point. When the temperature is below 6.0, the curve crossing is avoided and the distance becomes larger for lower temperatures at any given time. In addition, an oscillating feature appears and there exist

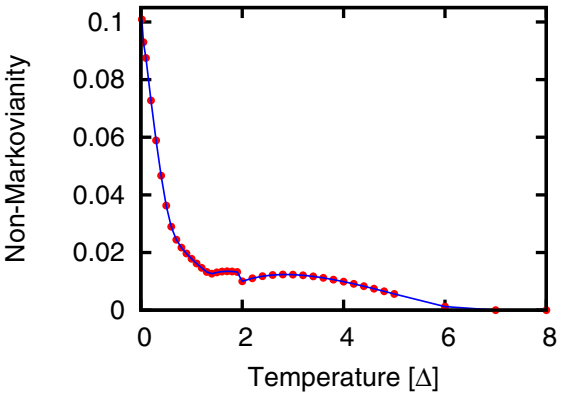


FIG. 5. (Color online) Temperature dependence of the non-Markovianity of the trajectory, starting from the left state. Filled circles are calculated results and the line is a guide for the eye. The temperature is in units of the tunneling frequency $\Delta$.

time intervals of increasing distinguishability. But these trends are reversed for temperatures above 6.0.

The calculated results for the maximum deviation from Markovianity $\mathcal{N}$ is shown in Fig. 5. Compared to those that do not invoke symmetry, the differences are always less than 0.2%, which again confirms the reliability of the symmetry preservation of the current method. Please bear in mind that we are using the stochastic method for $T < 2$ and the HEOM for $T \geqslant 2$, and the $\sigma$ quantity is the derivative of the population. So the stochastic method will lead to a larger error and causes the discontinuity around $T = 2$. It is a surprise that $\mathcal{N}$ is not monotonically decreasing. Because the curve is decreasing for temperatures below $T = 1$ and is convex in the temperature range 2–5, there must be a turning point between $T = 1$ and $T = 2$. This conclusion holds regardless of the errors of the stochastic simulation.

## IV. SUMMARY

We have developed an exact Hermitian SME to solve the quantum dissipative dynamics for the Caldeira-Leggett model. Within this framework the effect of a bath is represented by two correlated real-valued Gaussian noises. The current SDE is NMQSD in nature and valid at arbitrary temperatures. Compared to the approach suggested by Strunz *et al.*, the current SDE does not have a kernel to be determined. Though the structure of the SDE is exactly the same as that proposed by Stockburger *et al.* [22] and Shao [20], substantial differences exist. The original equation is non-Hermitian and requires three real noises, while the current one is Hermitian and involves only two real noises. The hermicity and lower number of noises greatly improve the numerical performance.

Because the only quantity required for the SME to simulate dissipative dynamics is the expectation of its solution, the coefficient of the $\delta$ function can be arbitrarily chosen as long as the correlation function is semipositive definite. This feature helps to improve the numerical efficiency. Tests with the HEOM at high temperatures and with symmetry preservation for a symmetric TLS show that the Hermitian SDE gives accurate results. Then stochastic simulations over a broad temperature range are performed and show that the Rabi frequency shifts with temperature.

Based on the symmetry property of the symmetric TLS we have proposed the matrix distance between one state and its symmetric counterpart as a measure of the non-Markovianity of a quantum state, which essentially provides a lower bound for the measure using the method of Breuer, Laine, and Piilo. This method measures the non-Markovianity with propagation starting from only one quantum state, without the need for complete knowledge of the quantum map. It will be appreciated in cases where the accurate non-Markovianity for the whole reduced system is not required and the existence of non-Markovianity of a particular process is of concern in the presence of symmetry. Combined with the Hermitian non-Markovian SME, the application of this idea is exemplified numerically for the dissipative symmetric TLS. It is interesting to learn that the maximum deviation from Markovianity does not decrease monotonically with increasing temperature for this system.

## ACKNOWLEDGMENTS

We are grateful to Professor Jiushu Shao for the suggestion to use the complex-valued Wiener process to solve the trace of the bath and for other helpful discussions. This work was supported by the National Natural Scientific Foundation of China (Grant No. 21373064), Program for Innovative Research Team of Guizhou Province (Grant No. QKTD[2014]4021), the Construction Project for Guizhou Provincial Key Laboratories (Z[2013]4009), and Natural Scientific Foundation, Guizhou Provincial Department of Education (Grants No. QJKY[2013]142, No. QJTD[2013]16, and No. ZDXK[2014]18). All calculations were performed at Guizhou Provincial High-Performance Computing Center of Condensed Materials and Molecular Simulation at Guizhou Normal College.

[1] P. Hamm, M. Lim, and R. M. Hochstrasser, Phys. Rev. Lett. **81**, 5326 (1998).
[2] G. S. Engel, T. R. Calhoun, E. L. Read, T.-K. Ahn, T. Mancal, Y.-C. Cheng, R. E. Blankenship, and G. R. Fleming, Nature **446**, 782 (2007).
[3] B.-H. Liu, L. Li, Y.-F. Huang, C.-F. Li, G.-C. Guo, E.-M. Laine, H.-P. Breuer, and J. Piilo, Nat. Phys. **7**, 931 (2011).
[4] M. M. Wolf, J. Eisert, T. S. Cubitt, and J. I. Cirac, Phys. Rev. Lett. **101**, 150402 (2008).
[5] S. Luo, S. Fu, and H. Song, Phys. Rev. A **86**, 044101 (2012).
[6] W.-M. Zhang, P.-Y. Lo, H.-N. Xiong, M. W.-Y. Tu, and F. Nori, Phys. Rev. Lett. **109**, 170402 (2012).
[7] S. Lorenzo, F. Plastina, and M. Paternostro, Phys. Rev. A **88**, 020102 (2013).

[8] Á. Rivas, S. F. Huelga, and M. B. Plenio, Phys. Rev. Lett. **105**, 050403 (2010).
[9] H.-P. Breuer, E.-M. Laine, and J. Piilo, Phys. Rev. Lett. **103**, 210401 (2009).
[10] C. Benedetti, M. G. A. Paris, and S. Maniscalco, Phys. Rev. A **89**, 012114 (2014).
[11] A. Caldeira and A. Leggett, Ann. Phys. **149**, 374 (1983).
[12] D. Alonso and I. de Vega, Phys. Rev. A **75**, 052108 (2007).
[13] B. Vacchini and H.-P. Breuer, Phys. Rev. A **81**, 042103 (2010).
[14] A. Smirne and B. Vacchini, Phys. Rev. A **82**, 022110 (2010).
[15] V. G. Morozov, S. Mathey, and G. Röpke, Phys. Rev. A **85**, 022101 (2012).
[16] R. Feynman and F. Vernon Jr., Ann. Phys. **24**, 118 (1963).
[17] I. Percival, *Quantum State Diffusion* (Cambridge University Press, Cambridge, 1998).
[18] C. H. Mak and R. Egger, Adv. Chem. Phys. **93**, 39 (1996).
[19] N. Makri, J. Math. Phys. **36**, 2430 (1995).
[20] J. Shao, J. Chem. Phys. **120**, 5053 (2004).
[21] J. T. Stockburger and C. H. Mak, Phys. Rev. Lett. **80**, 2657 (1998).
[22] J. T. Stockburger and H. Grabert, Phys. Rev. Lett. **88**, 170407 (2002).
[23] W. Koch, F. Großmann, J. T. Stockburger, and J. Ankerhold, Phys. Rev. Lett. **100**, 230402 (2008).
[24] Y.-A. Yan, F. Yang, Y. Liu, and J. Shao, Chem. Phys. Lett. **395**, 216 (2004).
[25] M. Schröter, S. Ivanov, J. Schulze, S. Polyutov, Y. Yan, T. Pullerits, and O. Kühn, Phys. Rep. **567**, 1 (2015).
[26] Y. Tanimura and R. Kubo, J. Phys. Soc. Japan **58**, 101 (1989).
[27] L. Diósi and W. T. Strunz, Phys. Lett. A **235**, 569 (1997).
[28] L. Diósi, N. Gisin, and W. T. Strunz, Phys. Rev. A **58**, 1699 (1998).
[29] W. T. Strunz, L. Diósi, and N. Gisin, Phys. Rev. Lett. **82**, 1801 (1999).
[30] W. T. Strunz, L. Diósi, N. Gisin, and T. Yu, Phys. Rev. Lett. **83**, 4909 (1999).
[31] T. Yu, Phys. Rev. A **69**, 062107 (2004).
[32] X. Zhao, J. Jing, B. Corn, and T. Yu, Phys. Rev. A **84**, 032101 (2011).
[33] J. Jing, X. Zhao, J. Q. You, and T. Yu, Phys. Rev. A **85**, 042106 (2012).
[34] W. T. Strunz and T. Yu, Phys. Rev. A **69**, 052115 (2004).
[35] T. Yu, L. Diósi, N. Gisin, and W. T. Strunz, Phys. Rev. A **60**, 91 (1999).
[36] A. J. Leggett, S. Chakravarty, A. T. Dorsey, M. P. A. Fisher, A. Garg, and W. Zwerger, Rev. Mod. Phys. **59**, 1 (1987).
[37] P. E. Kloeden and E. Platen, *Numerical Solution of Stochastic Differential Equations*, 2nd ed. (Springer-Verlag, Berlin, 1995).
[38] G. Chan and A. T. A. Wood, Stat. Comp. **9**, 265 (1999).
[39] Y.-A. Yan and Y. Zhou, Hyshe (hybrid stochastic-hierarchical equations); http://nano.gznc.edu.cn/~yunan/hyshe.html (2012).
[40] Y. Zhou, Y. Yan, and J. Shao, Europhys. Lett. **72**, 334 (2005).
[41] Y.-A. Yan and O. Kühn, New J. Phys. **14**, 105004 (2012).
[42] Y.-A. Yan and S. Cai, J. Chem. Phys. **141**, 054105 (2014).
[43] R. Barends, J. Baselmans, J. Hovenier, J. Gao, S. Yates, T. Klapwijk, and H. Hoevers, IEEE Trans. Appl. Supercond. **17**, 263 (2007).
[44] S. Kumar, J. Gao, J. Zmuidzinas, B. A. Mazin, H. G. LeDuc, and P. K. Day, Appl. Phys. Lett. **92**, 123503 (2008).
[45] X. Fu, X. Xi, K. Bi, and J. Zhou, Appl. Phys. Lett. **103**, 211108 (2013).
[46] W. A. Phillips, Rep. Prog. Phys. **50**, 1657 (1987).
[47] J. Gao, M. Daal, A. Vayonakis, S. Kumar, J. Zmuidzinas, B. Sadoulet, B. A. Mazin, P. K. Day, and H. G. Leduc, Appl. Phys. Lett. **92**, 152505 (2008).
[48] S. C. Hou, X. X. Yi, S. X. Yu, and C. H. Oh, Phys. Rev. A **83**, 062115 (2011).
[49] E.-M. Laine, J. Piilo, and H.-P. Breuer, Phys. Rev. A **81**, 062115 (2010).
[50] A. K. Rajagopal, A. R. Usha Devi, and R. W. Rendell, Phys. Rev. A **82**, 042107 (2010).
[51] S. C. Hou, X. X. Yi, S. X. Yu, and C. H. Oh, Phys. Rev. A **86**, 012101 (2012).
[52] Z. He, C. Yao, Q. Wang, and J. Zou, Phys. Rev. A **90**, 042101 (2014).
[53] D. Chruściński, A. Kossakowski, and Á. Rivas, Phys. Rev. A **83**, 052128 (2011).
[54] L. Mazzola, E.-M. Laine, H.-P. Breuer, S. Maniscalco, and J. Piilo, Phys. Rev. A **81**, 062120 (2010).
[55] Á. Rivas, S. F. Huelga, and M. B. Plenio, Rep. Prog. Phys. **77**, 094001 (2014).